Detection and identification of explosives using terahertz pulsed spectroscopic imaging

Y. C. Shen,[a] T. Lo, P. F. Taday, B. E. Cole, W. R. Tribe, and M. C. Kemp
TeraView Limited, Platinum Building, St John's Innovation Park, Cambridge CB4 0WS, United Kingdom

(Received 6 December 2004; accepted 3 May 2005; published online 9 June 2005)

The absorption spectrum of the explosive 1,3,5-trinitro-1,3,5-triazacyclohexane (RDX) has been measured using a conventional Fourier transform infrared spectroscopy and by terahertz pulsed spectroscopy. Seven absorption features in the spectral range of 5–120 cm^{-1} have been observed and identified as the fingerprint of RDX. Furthermore, the spatial distribution of individual chemical substances including RDX, has been mapped out using *reflection* terahertz spectroscopic imaging in combination with component spatial pattern analysis. This is the terahertz spectroscopy and chemical mapping of explosives obtained using *reflection* terahertz measurement, and represents a significant advance toward developing a terahertz pulsed imaging system for security screening of explosives. © *2005 American Institute of Physics*. [DOI: 10.1063/1.1946192]

Terahertz pulsed spectroscopy and imaging have been identified as very promising new techniques for the detection of explosives and other threats in security screening at airports and elsewhere. The terahertz region of the electromagnetic spectrum (0.3–10 THz or 10–300 cm^{-1}) has a unique combination of properties in that terahertz waves can propagate through barrier materials, such as clothing and common packaging materials; many substances show characteristic spectral features in the terahertz region; and the radiation is nonionizing and does not give rise to safety concerns.[1,2] At higher frequencies in the fingerprint region of the midinfrared, absorption and scattering limit the penetration through barrier materials. At frequencies lower than 300 GHz (10 cm^{-1}), there are no characteristic phonon vibrational modes in solids which can be used for material identification.

In an earlier paper, Kemp *et al.*[3] reported measurements showing spectral features in a number of common energetic substances including 1,3,5-trinitro-1,3,5-triazacyclohexane (RDX), tetranitro-tetracyclooctane (HMX), pentaerythritol (PETN), and trinitrotoluene (TNT). They also showed that commercial explosives based on these materials, such as PE-4 and Semtex, show the spectral features of their constituent explosives. Subsequently, Yamamoto *et al.*[4] reported the refractive index and absorption coefficient spectrum of RDX validating the results of Kemp *et al.*,[3] although the absorption spectrum of RDX reported by Cook *et al.*[5] showed some discrepancies. In all of these studies,[3–5] terahertz pulsed spectroscopy, performed in transmission mode, was used. Despite the dynamic range of the terahertz pulsed spectroscopy technique, crystalline materials, such as RDX, have a very high absorption coefficient and any practical implementation of a security system will need to use reflection rather than transmission.

In this work, we first measured the terahertz absorption spectrum of RDX using terahertz pulsed transmission spectroscopy and far-infrared Fourier transform infrared (FTIR) transmission spectroscopy. We then used a terahertz pulsed spectroscopy system operating in reflection and were able to observe the corresponding spectral features. Furthermore, terahertz spectroscopic images have been obtained using a terahertz pulsed imaging (TPI) system operating in reflection. Using component spatial pattern analysis,[6] the chemical distribution of RDX has been mapped out and distinguished from other substances. This is the first terahertz spectroscopy and chemical mapping of explosives ever realized using *reflection* terahertz measurements, and represents a significant advance toward developing a practical terahertz system for security screening of explosives.

To demonstrate that terahertz technology can be used for detecting RDX explosive, we first measured the terahertz absorption spectrum of RDX using a transmission terahertz spectrometer (TPI™ spectra 1000, TeraView Ltd., UK). The sample used here is a RDX pellet (13 mm diameter and 3 mm thickness) comprised of 30 mg RDX powder and 300 mg high-density polyethylene (PE) (particle size <80 μm, Chesham Chemicals, UK). The PE powder acts as a pellet binder and has low terahertz absorption. Figure 1(a) shows the amplitude of the Fourier transform of the terahertz wave form measured in the presence of a PE pellet [curve 1 of Fig. 1(a)] and the RDX pellet [curve 2 of Fig. 1(a)]. It is clear that the fast Fourier transform (FFT) amplitude of the measured terahertz signal, after propagating through the RDX pellet, decreases dramatically due to the strong absorption of RDX. The absorption spectrum of RDX was then calculated[7–13] using the PE pellet as a reference. As shown in Fig. 1(b), seven absorption features centered at 27.2, 34.9, 46.0, 51.8, 65.5, 74.2, and 105.5 cm^{-1} were found in the spectral range of 5–120 cm^{-1}. Note that our results reported in this letter agree very well with those of Yamamoto *et al.*[4] but cover an extended spectral range.

For comparison, a RDX pellet sample was further examined using a IFS113V FTIR spectrometer (Bruker Inc., Germany). As shown in Fig. 1(b), the absorption spectral features obtained with FTIR and terahertz pulsed spectroscopy agree very well, illustrating the reproducibility of the observed spectral features of RDX across different instrumentations. Note that due to the weak far-infrared light source, the signal-to-noise ratio drops dramatically below 20 cm^{-1} even with a liquid-helium-cooled silicon bolometer as a detector. Furthermore, we found that the best overall performance in spectral range of 1–100 cm^{-1} was obtained using a 23 μm Mylar beam splitter, although the interference pattern

[a]Electronic mail: yaochun.shen@teraview.com

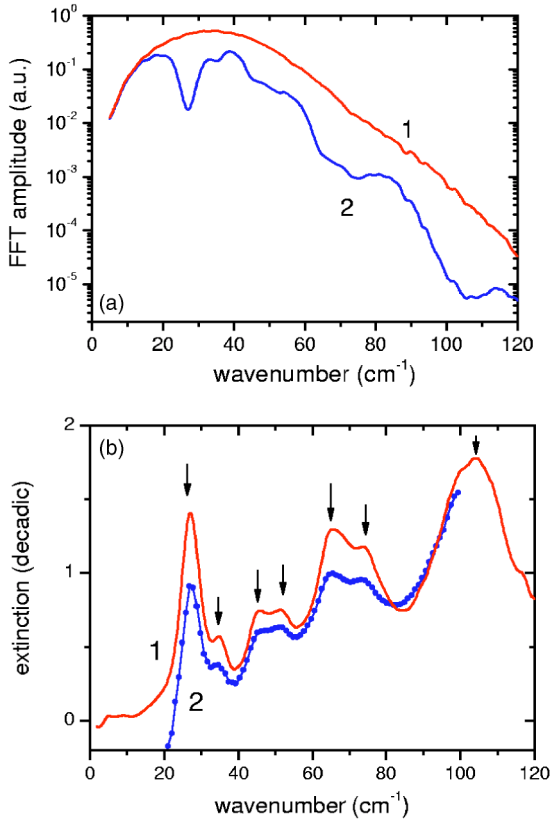

FIG. 1. (a) Fourier transform amplitude of the measured terahertz waveform after transmitting through a PE pellet (curve 1) and a RDX pellet (curve 2). (b) Absorption (power) spectrum of RDX pellet measured using a terahertz pulsed spectrometer (curve 1) and a FTIR spectrometer (curve 2).

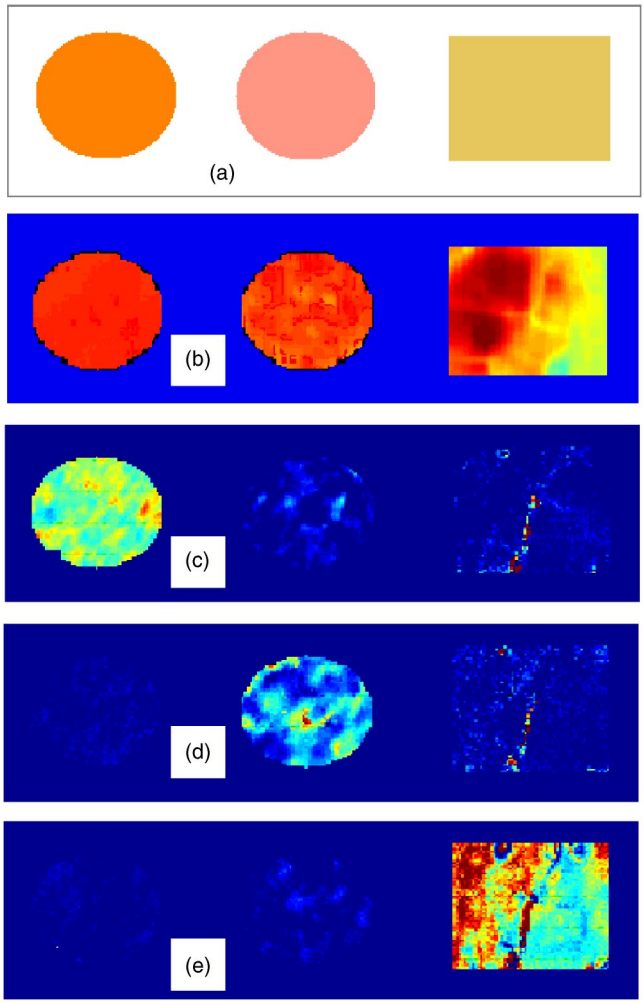

FIG. 2. (Color online) Schematic diagram of the sample (a), and its terahertz time-domain image (peak amplitude) (b). False-color terahertz chemical maps showing the spatial distributions of lactose (c), sucrose (d), and RDX (e).

from such a beam splitter gives an intensity valley of around 120 cm^{-1}.

To demonstrate the capability of TPI for detecting and identifying explosives, we prepared a sample comprised of a pure lactose pellet, a pure sucrose pellet, and a small piece of RDX-based sheet explosive. The pellets were formed by compressing lactose powder (Sigma-Aldrich, UK) (particle size $<100\ \mu m$) and sucrose powder (Sigma-Aldrich, UK) (particle size $\sim 500\ \mu m$), under 2 tons using a hydraulic press (Specac, UK). In the reflection measurement, we used a TPI™ scan imaging system (TeraView Ltd., UK), operating in a rapid scan mode. Terahertz maps were obtained by raster scanning the terahertz beam across the sample [Fig. 2(a)], which was mounted at the terahertz focus position. The scanned area was 8 mm $\times$ 24 mm, which corresponds to 80 $\times$ 240 pixels at 100 μm spacing. The total measurement time was about 16 min.

Figure 2(b) shows measured terahertz maps of the sample, generated by using the peak amplitude of the measured terahertz wave forms. We see a uniform map in the lactose area, whereas we see some contrast in the sucrose area due to the relatively large sucrose particles present in the sucrose pellet. Unlike the lactose and sucrose pellets, whose surfaces are relative smooth, the piece of sheet explosive has a larger surface roughness, giving rise to more contrast, as shown in Fig. 2(b). However, from the time-domain terahertz map alone, we cannot tell if a specific area is lactose, sucrose, or the explosive.

For the purpose of detecting and identifying explosives, we first Fourier transformed the time-domain terahertz wave form, and then calculated the absorption spectrum for each pixel of the image. As an example, the inset of Fig. 3(a) shows the measured terahertz wave form reflected from the center of the RDX explosive, with Fig. 3(a) showing the amplitude spectrum of its Fourier transform. The main absorption feature of RDX at 27 cm^{-1} is clearly visible. The absorption coefficient $\alpha(v)$ and the refractive index $n(v)$, in the spectral range 5–80 cm^{-1} are then calculated as

$$\sqrt{\varepsilon} \equiv n(v) + j\frac{\alpha(v)}{4\pi v} = \frac{1 - E_S(v)/E_M(v)}{1 + E_S(v)/E_M(v)},$$

where v is the wave number, and $E_S(v)$ and $E_M(v)$ are the Fourier transform of the measured terahertz waveform reflected from a sample and a reference mirror, respectively. Figure 3(b) shows the first derivatives of the absorption coefficient of RDX explosive. As expected, the first derivative spectrum measured in reflection mode [curve labeled "1" in Fig. 3(b)] is the same as that measured in transmission mode [curve labeled "2" in Fig. 3(b)]. We believe that these results represent the first *measured* terahertz reflection spectrum of RDX. We note that Yamamoto *et al.*[4] mentioned the usefulness of the reflection spectra in the detection of thick explosives, and also calculated the reflection spectra from the

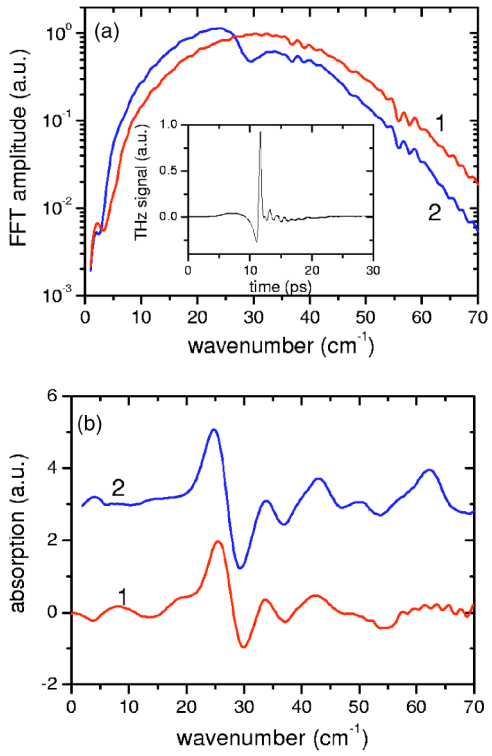

FIG. 3. (a) Fourier transform amplitude of the measured terahertz waveforms after reflecting from a PE pellet (curve 1) and a piece of RDX explosive (curve 2). The inset show the terahertz wave form measured for RDX explosive. (b) The first derivative absorption spectrum of RDX explosive obtained from a reflection measurement (curve 1) and a transmission measurement (curve 2).

complex refractive index measured by their transmission measurement.

We then calculated the absorption spectrum for all pixels of the terahertz map, each in the same manner as discussed above. This generated a three-dimensional data set where two axes describe vertical and horizontal spatial dimensions, and the third axis represents the spectral frequency dimension. These images contain comprehensive information on both the spatial and chemical distribution of the sample.

In order to extract the spatial distributions of individual chemical substances in the sample, we first compress the three-dimensional data set to a two-dimensional matrix F_{NL}, where L is the number of pixels ($L=80\times240$) and N is the number of frequency components ($N=512$). If we assume that the sample has M chemical substances ($M=3$ for the present case) and each chemical substance has a known absorption spectrum with N frequency components, we then have a featured spectral matrix of S_{NM}. The spatial distribution of individual chemical substances in the sample is then calculated using the component spatial pattern analysis method[6] as

$$[P_{ML}]=([S_{NM}]^t[S_{NM}])^{-1}[S_{NM}]^t[F_{NL}],$$

where P_{ij} represents the probability of the occurrence of the ith substance ($i=1$ for lactose, $i=2$ for sucrose, and, $i=3$ for RDX) at the jth pixel ($j=1,2,\ldots,L$, and $L=80\times240$). Note that the featured spectral matrix, S_{NM}, which forms the basis for chemical mapping analysis, can be obtained from reflection or transmission terahertz spectroscopic measurements, or even from principal components analysis of independent terahertz spectroscopic imaging measurements.

Figures 2(c) and 2(d) show the chemical mapping terahertz maps reconstructed using $P_{1j}(j=1,2,\ldots,L)$. As expected, P_{1j} has large values across the entire lactose pellet [left of Fig. 2(c)], while P_{1j} is close to zero across the sucrose pellet [middle of Fig. 2(c)] and the RDX explosive (right of Fig. 2(c)]. Similar discriminations are made in the terahertz maps constructed using P_{2j} and $P_{3j}(j=1,2,\ldots,L)$, which correspond to spatial distributions of sucrose and RDX, respectively [Figs. 2(d) and 2(e)].

For practical security screening applications, we can construct a spectral matrix S_{NM} comprised of terahertz spectra of known explosives. We can then apply this spectral matrix to terahertz maps of an unknown object. Any bright spot/area in the reconstructed chemical map may indicate the possible presence of explosive. For example, after applying the terahertz spectrum of RDX to analyzing the terahertz spectroscopic maps, only the area containing RDX is highlighted [see Fig. 2(e)] demonstrating that TPI has the specificity for detecting and identifying explosives, such as RDX.

We note that Watanabe *et al.*[6] first demonstrated the nondestructive terahertz mapping of illicit drugs using spectral fingerprints at seven discrete frequencies measured in transmission. The TPI system used in our experiments has a broadband spectral coverage of 10–80 cm^{-1} (0.3–2.4 THz). This spectral range enables us to map out precisely, from a single measurement, the spatial distribution of an individual chemical substance in a multichemical sample. The high absorption coefficient of the body and explosive precludes the use of conventional transmission spectroscopy systems. However, as demonstrated in this letter, the terahertz reflection spectroscopy—when coupled with modern analytical methods—provides a practical solution. In conclusion, we have demonstrated the capability of terahertz spectroscopy for detecting and identifying explosives and for the chemical mapping of the spatial distribution of individual chemicals in a sample. It represents a significant advance toward developing a TPI system for security screening of explosives.

Parts of this work were carried out under contract for the UK Government whose support is gratefully acknowledged.

[1] J. Yinon and S. Zitrin, *Modern Methods and Applications in Analysis of Explosives* (Wiley, Chichester, 1993).
[2] T. Gozani, R. E. Morgado and C. C. Seher, J. Energ. Mater. **4**, 377 (1986).
[3] M. C. Kemp, P. F. Taday, B. E. Cole, J. A. Cluff, A. J. Fitzgerald, and W. R. Tribe, Proc. SPIE **5070**, 44 (2003).
[4] K. Yamamoto, M. Yamaguchi, F. Miyamaru, M. Tani, M. Hangyo, T. Ikeda, A. Matsushita, K. Koide, M. Tatsuno, and Y. Minami, Jpn. J. Appl. Phys., Part 2 **43**, L414 (2004).
[5] D. J. Cook, B. K. Decker, G. Maislin, and M. G. Allen, Proc. SPIE **5354**, 55 (2004).
[6] Y. Watanabe, K. Kawase, T. Ikari, H. Ito, Y. Ishikawa, and H. Minamide, Appl. Phys. Lett. **83**, 800 (2003).
[7] B. Ferguson and X.-C. Zhang, Nat. Mater. **1**, 26 (2002).
[8] M. C. Beard, G. M. Turner, and C. A. Schmuttenmaer, J. Phys. Chem. B **106**, 7146 (2002).
[9] T. D. Dorney, R. G. Baraniuk, and D. M. Mittleman, J. Opt. Soc. Am. A **18**, 1562 (2001).
[10] M. Walther, B. Fischer, M. Schall, H. Helm, and P. Uhd Jepsen, Chem. Phys. Lett. **332**, 389 (2000).
[11] M. Walther, B. M. Fischer, and P. Uhd Jepsen, Chem. Phys. **288**, 261 (2003)
[12] Y. C. Shen, P. C. Upadhya, A. G. Davies, and E. H. Linfield, Appl. Phys. Lett. **82**, 2350 (2003).
[13] P. F. Taday, I. V. Bradley, D. D. Arnone, and M. Pepper, J. Pharm. Sci. **92**, 831 (2003).